GLOBAL DISTRIBUTION AND SPECTRAL PROPERTIES OF LOW-REFLECTANCE MATERIAL ON MERCURY. Rachel L. Klima (Rachel.Klima@jhuapl.edu)[1], David T. Blewett[1], Brett W. Denevi[1], Carolyn M. Ernst[1], Elizabeth A. Frank[2], James W. Head, III[3], Noam R. Izenberg[1], Scott L. Murchie[1], Larry R. Nittler[2], Patrick N. Peplowski[1], and Sean C. Solomon[2,4]. [1]Johns Hopkins University Applied Physics Laboratory, Laurel, MD 20723, USA; [2]Carnegie Institution of Washington, Washington, DC 20015, USA; [3]Brown University, Providence, RI 02912, USA; [4]Lamont-Doherty Earth Observatory, Columbia University, Palisades, NY 10964, USA.

Introduction: Distinctive low-reflectance material (LRM) was first observed on Mercury in Mariner 10 flyby images [1]. Visible to near-infrared reflectance spectra of LRM exhibit a flatter slope than the average reflectance for Mercury, which is strongly red sloped (increasing in reflectance with wavelength). Moreover, LRM is lower in reflectance (<0.04–0.05 at 560 nm wavelength) than an already dark planet (global average 0.06–0.07) [2]. In some cases, LRM spectra also exhibit a curvature suggestive of a weak, broad absorption band near 600 nm [2,3]. From Mariner 10 and early MErcury, Surface, Space, ENvironment, GEochemistry, and Ranging (MESSENGER) flyby observations, it was suggested that ilmenite, ulvöspinel, carbon, or iron metal could cause the characteristic dark, flat spectrum of LRM and the global darkening of Mercury [1,2]. However, once MESSENGER entered orbit, low iron and titanium abundances measured by the X-Ray Spectrometer and Gamma-Ray Spectrometer ruled out ilmenite and ulvöspinel as important constituents and implied a different darkening phase, such as carbon or small amounts of opaque minerals dispersed as micro- or nanophase particles in a silicate matrix [3-5]. To test the various hypotheses for the mineral composition and origin of the darkening agent in LRM and on Mercury more generally, we present a global map of the distribution of LRM across Mercury.

Mapping Low-Reflectance Material: Low-reflectance material is defined by its color and reflectance and is not typically associated with morphological features other than ejecta deposits. The low ferrous iron content of Mercury's surface results in a lack of the spectral absorption bands typically used to map minerals. Nonetheless, mathematical transformations such as principal component (PC) analysis can tease apart subtle spectral differences in the color data measured by the Mercury Dual Imaging System (MDIS). Both PC2 and PC3 exhibit spectral trends in which LRM is an endmember. Shown in Fig. 1 is a color composite of Mercury with LRM, here defined as material with a 560 nm reflectance <4.8% and with a PC2 value within the lowest 20% of the full range of the surface, highlighted in magenta. LRM can also be seen as black material in the PC3 map, as illustrated in Fig. 2.

Low-reflectance material is primarily associated with crater and basin ejecta. There are some regional concentrations where many moderate sized craters or several larger basins excavated LRM in close proximity to one another. Low-reflectance material is most immediately recognizable visually when excavated by craters and deposited onto high-reflectance red plains (HRP, as in Caloris basin), due to the contrasting reflectance and spectral shapes of the different stratigraphic layers. However, it is also abundant throughout older, rougher terrains, where its boundaries are more difficult to delineate as they grade into low-reflectance blue plains (LBP). In these older terrains LRM is still apparently associated with crater ejecta, but the high density of craters excavating LRM results in a patchy distribution of low-reflectance, low-PC2 material.

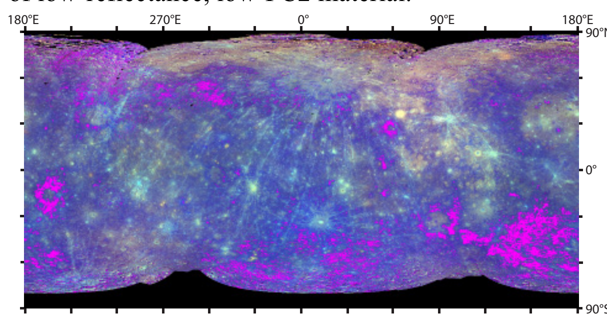

Fig. 1. MDIS color mosaic in which red represents PC2, green PC1, and blue the ratio of the 430-nm/1000-nm reflectance. LRM deposits are in magenta. Simple cylindrical projection.

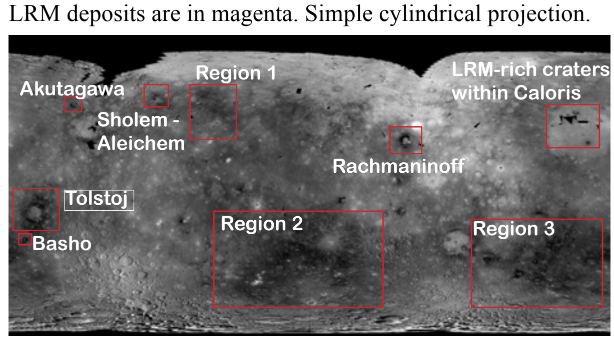

Fig. 2. PC3 map with the locations of regions for which spectral data have been extracted. Simple cylindrical projection.

There is no clear global relationship between crater size and excavation of LRM. LRM-rich ejecta are found surrounding craters from <100 km in diameter through basins larger than 700 km across. On a local scale, within Caloris basin, LRM has been determined to be buried by about 2.5 km of plains material and to extend to at least 11 km depth [6]. Tolstoj, a basin 360 km in diameter, excavated large amounts of LRM, as did the slightly smaller Rachmaninoff, suggesting that LRM is present up to at least ~20 km depth at some locations.

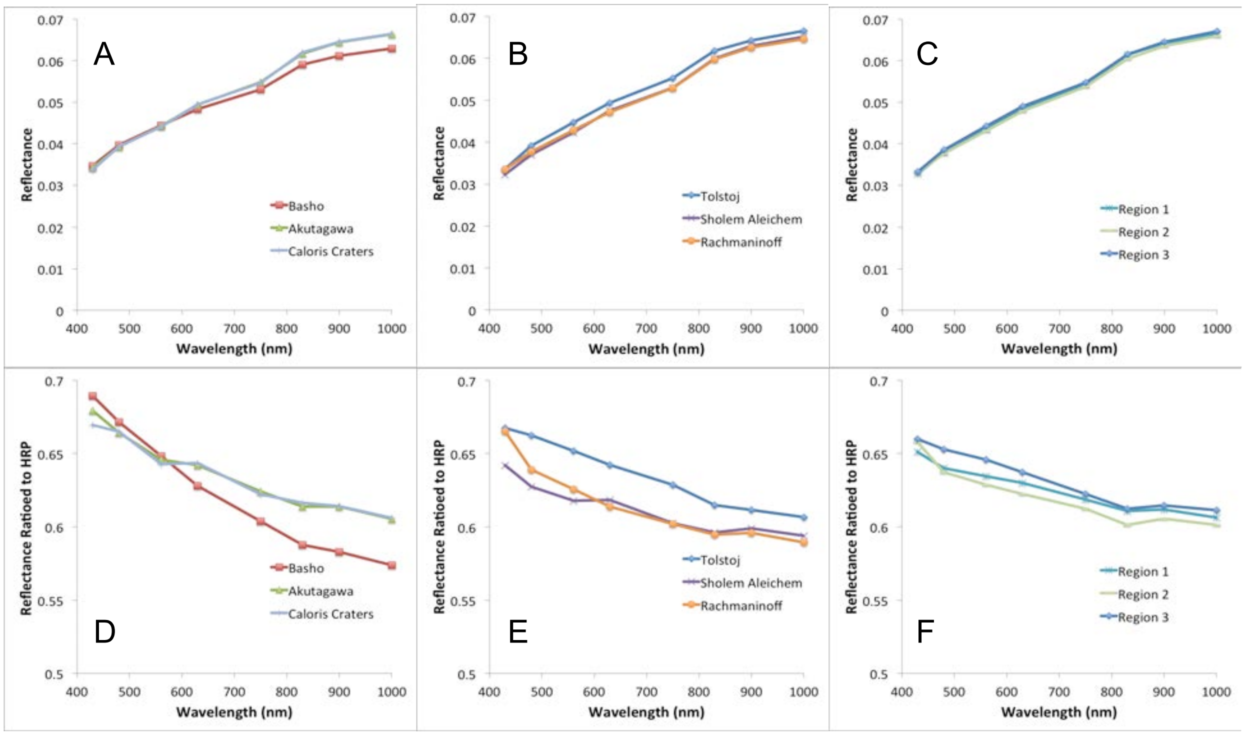

Fig. 3. Averaged LRM reflectance and ratioed reflectance spectra from (A,D) moderate-sized (~100-km-diameter), relatively fresh craters, (B,E) large craters and basins (200-400 km diameter), and (C,F) broad surface regions. The lower row shows the same spectra ratioed to a spectrum of the high-reflectance plains (HRP) to accentuate spectral shape.

The largest regional expanse of LRM occurs south of Caloris basin. The most concentrated deposits of LRM within this region (here termed Region 3) are associated with moderate-sized (~100-km-diameter) craters, though the entire region is LRM-rich. This area is also the most heavily cratered terrain on Mercury [7, 8], perhaps indicating that the LRM source region here is most shallow.

Spectral Properties of LRM: To determine the average spectral properties of major LRM deposits as measured by MDIS, we examine average spectra from several LRM-rich example locations (Fig. 2). Thermal neutron measurements for three of the regions, Akutagawa crater (106 km diameter), Sholem-Aleichem crater (195 km diameter), and Region 1, are consistent with 1-3 wt% enhancement in carbon over the global abundance [9], consistent with the hypothesis that the darkening agent in LRM is carbon [3, 10]. The spectra from these regions are shown in Fig. 3, both as reflectance and as reflectance ratioed to an HRP spectrum to accentuate the spectral slope and curvature relative to younger volcanic terrains on Mercury. Subtle differences can be seen in the spectra of Basho, Rachmaninoff, and Sholem-Aleichem. The spectral character of Tolstoj is similar to the broader regional expanses of LRM, whereas younger craters exhibit a slightly bluer slope and a more prominent broad depression near 600 nm, consistent with laboratory spectra of graphite [3]. Basho, the freshest of these craters on the basis of crater rays and obvious secondaries, exhibits the bluest slope of all regions and craters examined.

Summary: Low-reflectance material most often shows clear evidence of having been excavated from depth. In cases where it is not clearly associated with specific craters, it occurs in patchy spots within broad regions where the ejecta from numerous small craters overlap. Were the LRM source region present as a uniform global layer, it would need to be far greater than 10 km thick to account for excavation by both small craters and larger basins. The sporadic excavation of LRM instead argues for a discontinuous distribution within the crust, as previously suggested [9], or at least by different LRM burial depths. The three LRM regions measured by neutron spectrometry [9] are spatially and spectrally representative of the diversity of LRM observed globally. A ~600-nm absorption, potentially associated with graphite, is present in the fresher exposures of LRM. This evidence supports the presence of a graphite-rich subsurface, perhaps the remnants of a magma ocean floatation crust [11].

References: [1] Hapke, B. et al. (1975) JGR 80, 2431. [2] Robinson, M.S. et al. (2008) Science 321, 66. [3] Murchie, S.L. et al. (2015) Icarus 254, 287. [4] Nittler, L.R. et al., (2011) Science 333, 1847. [5] Evans, R.G. et al. (2012) JGR 117, E00L07. [6] Ernst, C.M. et al. (2015) Icarus 250, 413. [7] Fassett, C. I. et al. (2011) GRL 38, L10202. [8] Denevi B.W. et al., this volume. [9] Peplowski, P.N. et al. (2016) Nature Geosci., in press. [10] Bruck Syal, M. et al. (2015), Nature Geosci. 8, 352. [11] Vander Kaaden, K.E. and McCubbin, F.M. (2015) JGR Planets 120, 195.